# DETECTION OF LOW INSULATION AND UNBALANCE VOLTAGE IN THREE-PHASE INDUCTION MOTORS USING VIBRATION ANALYSIS UNDER DIFFERENT LOADS

**Jorge Nei Brito, brito@ufsj.edu.br**
**Paulo Cezar Monteiro Lamim Filho, lamim@ufsj.edu.br**
UFSJ - Federal University of São João del Rei, Praça Frei Orlando nº 170, Centro, São João del Rei - MG, (Brazil).

**Vinicius Augusto Diniz Silva, viniciusadsilva@gmail.com**
**Robson Pederiva, robson@fem.unicamp.br**
UNICAMP - University of Campinas, Postal Code 6051 - Campinas - SP, 13083-970, (Brazil).

***Abstract.*** *In this work the application of the vibration analysis for the detection and diagnosis of the low insulation between turns and unbalance voltage in the six poles three-phase induction motor under different loads (80, 90 and 100% of load) is proposed. The detection of faults through the comparison of spectra of vibration analysis when they are still in development phase makes possible to the maintenance engineer to plan a corrective action regarding the foreseen fault. The results showed the efficiency of the vibration technique and their relevance to detect and diagnose faults in different induction motors. In this way it is possible to include it in a maintenance programs*.

***Keywords****: fault detection, three-phase induction motors, low Insulation, unbalance voltage, vibration analysis*

## 1. INTRODUCTION

In the last twenty years several researches have been developed, aimed at detecting and diagnosing faults in three-phase induction motors, (Trutt and Cruz, 1993), (Henao *et al.* 2003), (Nakamura *et al.* 2008), (Lamim Filho 2007). Wang and Lai (1999) presents a discussion related to the modeling of the vibration behavior of an induction motor of 2.2 kW. The results show, that when modeling the vibration behavior of a motor structure, the laminated stator should be treated as an orthotropic structure and the teeth of the stator could be neglected. As an outer casing, end-shields support all affect of the vibration properties of the whole structure; these substructures should be incorporated in the model to improve accuracy.

Zanardelli *et al.* (2005) developed three wavelet-based methods (classification base on a decision tree; classification method based on a unit sphere and classification based on discriminate functions) for the prognosis of mechanical and electrical failures in electric motors for automobiles. Although all thee algorithms performed well, the second showed the best balance between easy implementation and accuracy, how it could adapt to different types of faults and few subjective decisions regarding its implementation were required. All three methods were implemented in a laboratory and then evaluated.

Widdler Jr. *et al.* (2006) presented an induction motor model for high-frequency torsional vibration analysis. Two torsional vibration models are developed. One model assumes the rotor to be rigid, while the other has a compatible rotor. The compatible model allows for greater transmission of high-frequency oscillations, and a better prediction of the measured output shaft vibration.

Wang *et al.* (2009) presented an innovative method to perform classification of fault signal without the use of preliminary extraction of the vector. By estimating the time delay and embedding dimension of time series, the vibration signal is reconstructed into phase space (RPS) and Gaussian mixture model (GMM) is established for every kind of fault signal in the reconstructed phase space.

After these models, the classification is made of the fault signal is performed, the computation of conditional probabilities of the signal in each GMM model and the selection of the model with the highest probability. By analyzing the vibration signal of different kinds of bearing status with different conditions, it is proved that this method is effective for classifying not only fault types, but also their severity.

Baccarini *et al.* (2010) proposed a dynamic model to analyze electrical and mechanical faults in induction machines and this includes asymmetries in the supply line and load conditions. According to the authors, the model allows to analyze the interactions between different faults in order to detect possible false alarms. Simulations and experimental results were performed to confirm the validity of the model.

However, one of the difficulties the researchers encountered is to distinguish faults such as: inter-turn short circuits, unbalanced voltage supplies and rotor eccentricity, (Lamim Filho, 2007) and (Silva, 2006).

The detection of faults by comparing the spectra of vibration analysis, when they are still in the development phase, enables the maintenance engineer to plan a corrective action regarding the foreseen fault.

The degradation of the insulation of electric motors can be accelerated if the motor operates in aggressive environments, turning it still more susceptible to incipient faults, (Lamim Filho, 2007) and (Benbouzid and Kliman, 2003).

If the incipient faults or the gradual deterioration are not detected, it can lead to breakage of the motor causing damages. Several faults can be avoided if the application, working condition and origin of the faults are understood, (Lamim Filho, 2007). In terms of electric motors, the reliability has been growing constantly due to the importance of their applications and technological progress.

In this work the application of the vibration analysis for the detection and diagnosis of the low insulation between turns and unbalance voltage in the six poles three-phase induction motor under different loads (80, 90 and 100% of load) which, in turn, represent the majority of the electrical failures in motors, is proposed, (Lamim Filho, 2007) and (Benbouzid and Kliman, 2003).

For a better understanding of the relationship failure/sign, conducting controlled experiments in a trial is indispensable. Thus, several experimental tests were done at the Laboratory of Vibration and Control of UNICAMP (University of Campinas). An experimental trial was carried out, where its robustness guaranteed the reproducibility of tests (inter-turn short circuits and voltage unbalance supplies) under the same conditions and different loads (80, 90 and 100% load).

## 2. EXPERIMENTAL TESTS

The experimental test, Fig. 1, was assembled in the Laboratory of Vibration and Control of the FEM-UNICAMP-Department of Mechanical Design. The faults were inserted in the six poles three-phase motors {1}, squirrel cage rotor, 5 CV, 220 V, 60 Hz, category N, 44 bars, 36 slots, SKF 6205-2Z bearing, ID-1, frame 100L, class of insulation B. A CC generator {4} fed by a resistance bank is used as a load system. By varying the excitation current of the CC generator field, it is possible, therefore, the variation of the motor load.

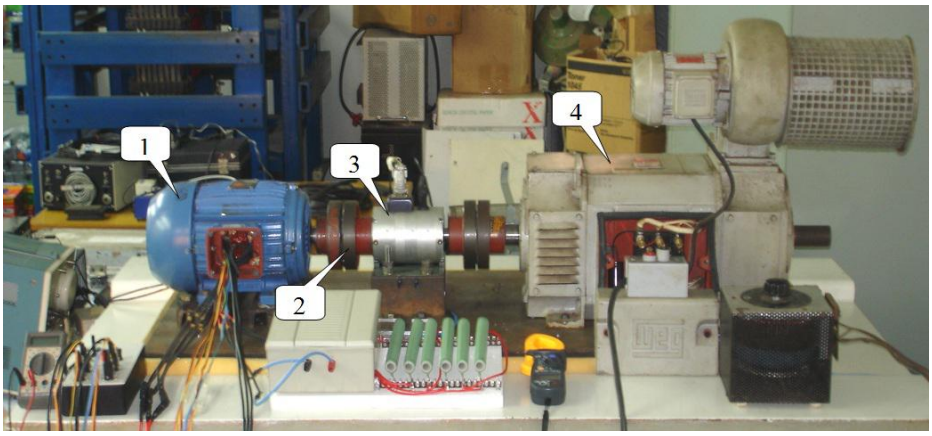


Figure 1. View of the experimental setup

The generator is connected to the electric motor through flexible couplings {2} and a torque wrench of S. Himmelstein and Company, model MCRT 9-02T, 0-7500 rpm, bi-directional and maximum toque of 1000 LB-IN {3} which served to ensure the same operating condition in all tests.

To simulate a low insulation among spirals from a same phase, it was extracted four derivations in a coil, Fig. 2a. Those derivations were placed externally and connected in series (two each) with a resistance bank, Fig. 2b, of 1 □, 100 Watts (each) connected in parallel and added to the circuit through a group of breakers in order to control the current intensity of short circuit in approximately 10 A, maintaining the nominal load of the motor.

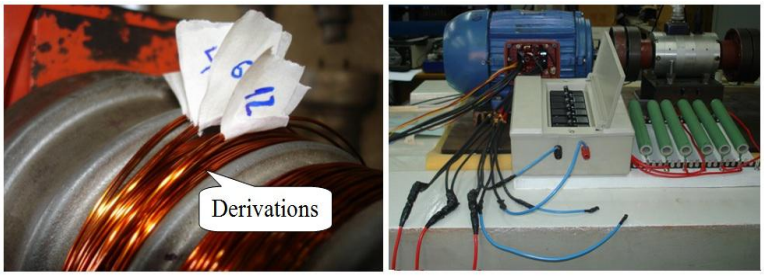


Figure 2. Recoiling of the induction motor: (a) Derivations in a coil, (b) Resistance bank.

The stator winding arrangement is illustrated in Fig. 3. The location of the tapings of one of the motor phases (phase A) is shown in Fig. 4.

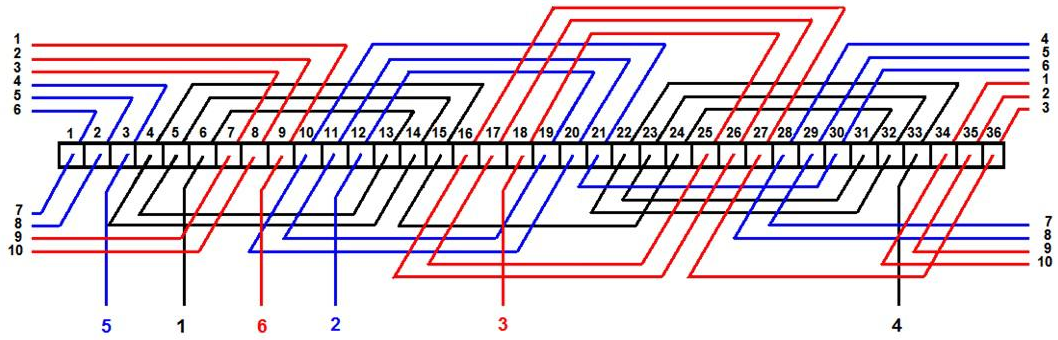


Figure 3. Stator winding arrangement.

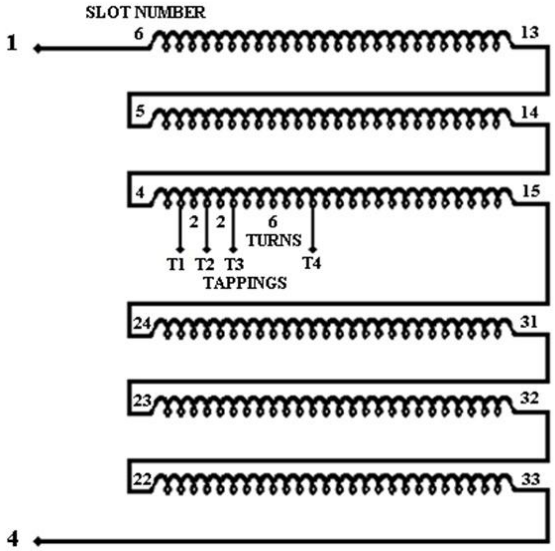


Figure 4.Location of the tapings for motor phase A.

Each coil is constituted by 26 coils with the wire gauge equal to 16 AWG. As each phase is formed by 6 spools, there are a total of 156 coils per phase.

Therefore, the configuration allows the analysis of low insulation (short circuit) between, at least, two turns and, in the maximum, 10 turns for the phase A corresponding to the percentages of 1.2% (2/156) and 6.4% (10/156) of low insulation. The excitation phase unbalance was obtained by inserting a variable resistance in series with one of the power-supplying phases of the electric motor, Fig. 5.

Figure 5. Excitement for unbalance phase.

## 3. GENERAL CONSIDERATIONS

The factors that affect the behavior of the induction motors can be grouped without problems of electric or magnetic origin and problems of mechanical origin. Due to the importance of understanding the sources of disturbances for fault diagnosis, several studies have been conducted in order to identify possible deterministic frequencies, (Lamim Filho, 2007), (Baccarini, 2005) and (Liu and Huang, 2005).

### 3.1. General Considerations on Unbalanced Voltage

Liang and Iwnicki (2003) conducted a study comparing vibration analysis, per-phase current and transient speed analysis for the detection of asymmetries in the stator and rotor faults in three-phase induction motors. It was shown that when the engine is subjected to a voltage unbalance, there is an increase in the characteristic frequency or failure (twice the value of the line frequency).

According to Dymond and Stranges (2007), the presence of voltage unbalance will affect losses, heating, noise, vibration, torsional pulsations, slip, shaft voltages and currents, and motor accelerating torque. The motor bar losses are increased and unbalanced stator currents result in uneven heating within stator phases. Unbalanced voltages also result in a torque pulsation at a frequency of 120 Hz , which may generate noise and vibration levels. The accelerating toque of the motor can be reduced somewhat if the machine is operated by unbalanced voltage sources.

The force acting on a conductor subjected to a magnetic field can be described by (Lamim Filho, 2007) as in Eq. (1) where $\vec{i}$ is the electric current vector $\vec{B}$ is the flux density vector and $l$ is the stator length.

$$F = \vec{i} \times \vec{B}\, l \tag{1}$$

If the three-phase stator winding of the induction motor is fed by a balanced sinusoidal voltage, a magnetic field is produced in the air gap which has sinusoidal distribution in space and rotates with synchronous speed *n1* while the rotor spins with velocity *n*. The difference between the two speeds is called slip speed.

The fundamental spatial component of the resulting air gap flux wave rotates the rotor with a slip speed $s_{n1}$ and induces an electromotive force (EMF) of slip frequency $s_f$ on the rotor circuit. These electromotive forces generate currents of slip frequency in the short-circuiting rotor bars. The rotor currents with slip frequency generate a magneto motive force (MMF) whose fundamental spatial frequency also moves at slip speed around the rotor. Superimposed on this rotation, *n* is the mechanical rotation of the motor. Thus, the speed of the rotor field in space is the sum of these two speeds (Baccarin, 2005).

Considering, first, failures in the rotor, the fundamental frequencies in the circuit are: line frequency *f*, frequency of rotor rotation $f_r$ and slip frequency $f_2$ ($f_2 = s_f$).

Analyzing the case of a uniform air gap (infinite number of slots) and a pure sinusoidal current, the expression for the force will have two components with slip frequency, but delayed by an angle $\theta$, as shown in Eq. (2).

$$F_{rotor} = k \sin(s\omega_1 t) \sin(s\omega_1 t - \theta) \tag{2}$$

Decomposing the product of sines we have Eq. (3) where $2s\omega_1 t = 2\omega_2 t = 2(2\pi f_2)t$.

$$F_{rotor} = \frac{k}{2}\left[\cos\theta - \cos(2s\omega_1 t - \theta)\right] \tag{3}$$

Equation (3) shows that the force generated has a constant and a variable part with frequency $2s_f$, that is, twice the slip frequency. As the irregularities are attributed to the rotating part of the induction motor, the unbalance caused by the MMF will unbalance the forces on both sides of the rotor, causing vibration. The vibrations induced on the frame of the engine are subject to the instantaneous angular position of the rotor. Multiplying (3) by cos (ωt), where ω is the motor speed, the radial projection of the rotational forces on the frame of the engine is obtained as shown in Eq. (4).

$$F_{rotor} = \frac{k}{2}\left[\cos\theta\cos\omega t - \cos(2s\omega_1 t - \theta)\cos\omega t\right] \tag{4}$$

Equation (4) is the expression of an amplitude modulation with a carrier, where the carrier frequency is the rotation frequency of the motor and the frequency of the modulation signal is twice the slip frequency. Due to the *AM* modulation, the mechanical vibration in the frame has the same harmonic content as the rotational force and in its

spectrum, the component with the same frequency as the rotor has side bands spaced with twice the slip frequency. If defects are located in the stator, the resulting forces do not rotate, as shown in the Eq. (5) and Eq. (6).

$$F_{stator} = k\sin(\omega_1 t)\sin(\omega_1 t - \theta) \tag{5}$$

$$F_{stator} = \frac{k}{2}\left[\cos\theta - \cos(2\omega_1 t - \theta)\right] \tag{6}$$

The resulting vibration has a constant component and one alternate with twice the frequency of the line. The frequency of rotation of the rotor and the slip frequency are also involved in the process and can cause modulations around twice the frequency of the line.

### 3.2. General Considerations on Short Circuits

According to Gojko and Penman (2000), for three-phase motor with n bars, the magneto motive force (MMF) frequency generated by the current that runs through a rotor cycle with maximum amplitude $I_{r\,max}$ can be found by Eq. (7) and Eq. (8), where $t$ is the time, $\theta_r$ is the angle of rotor position, $\omega_1$ is the mains angular frequency and $s$ is the rotor slip.

$$F_{loop1}(t,\theta_r) = \sum_{v=1}^{\infty}\left[K_v\cos(v\theta_r + s\omega_1 t) + K_v\cos(v\theta_r - s\omega_1 t)\right] \tag{7}$$

$$K_v = \frac{2}{v\pi}\left(1-\frac{1}{n}\right)\sin\left(v\frac{\pi}{n}\right)I_{r\max} \tag{8}$$

Equation (7) is obtained from a rotor reference frame. In the neighboring rotor loop, which is shifted by $2\pi/n$ *rad* in space, a current of the same frequency and amplitude but phase shifted by $p.2\pi/n$, where $p$ is the number of pole pairs. This loop produces its own MMF which has the following Eq. (9).

$$F_{loop2}(t,\theta_r) = \sum_{v=1}^{\infty}\left[K_v\cos\left(v\theta_r + s\omega_1 t - (v+p)\frac{2\pi}{n}\right) + K_v\cos\left(v\theta_r - s\omega_1 t - (v-p)\frac{2\pi}{n}\right)\right] \tag{9}$$

The total rotor MMF is the sum of the MMFs of all the rotor loops and it is given by Eq. (10).

$$F_r(t,\theta_r) = \sum_{i=0}^{n-1}\sum_{v=1}^{\infty}\left[K_v\cos\left(v\theta_r + s\omega_1 t - i.(v+p)\frac{2\pi}{n}\right) + K_v\cos\left(v\theta_r - s\omega_1 t - i.(v-p)\frac{2\pi}{n}\right)\right] \tag{10}$$

Equation (10) clearly shows that MMF waves exist only for the cases in which $v = p$, $v + p = \pm\lambda n$ and $v - p = \pm\lambda n$, $\lambda = 1, 2, 3\ldots$ As $v$ can only be a positive integer, it follows that only for $v = p$ and $v = \lambda n \pm p$ MMF waves exist. Therefore, apart from the basic harmonic of MMF for $v = p$, which is the armature reaction to the basic harmonic of MMF from the stator side, there exists the so-called rotor slot harmonics of order $\lambda n \pm p$ (space harmonics). These MMF waves have the Eq. (11) when observed from the stator side.

$$F_r(t,\theta) = F_{r1}\cos\left(\left(1-\lambda\frac{n}{p}(1-s)\right)\omega_1 t + (\lambda n - p)\theta\right) + F_{r2}\cos\left(\left(1+\lambda\frac{n}{p}(1-s)\right)\omega_1 t - (\lambda n + p)\theta\right) \tag{11}$$

Similarly, it can be shown that higher frequency rotor currents, which are a result of higher harmonic flux density waves from the stator side, produce MMF waves which have a similar shape given by Baccarini (2005).

Multiplying (11) and (12) MMF waves with constant air-gap permanent, the flux density waves of the same shape will be obtained. Flux-density waves will induce electromotive forces (EMFs) in the stator windings and these EMFs will generate currents.

$$F_{r\mu}(t,\theta) = \\ = F_{r\mu 1}\cos\left(\left(1-\lambda\frac{n}{p}(1-s)\right)\omega_1 t+(\lambda n-\mu p)\theta\right)+ \\ +F_{r\mu 2}\cos\left(\left(1+\lambda\frac{n}{p}(1-s)\right)\omega_1 t-(\lambda n+\mu p)\theta\right) \tag{12}$$

From Eq. (11) and Eq. (12) it is clear that besides the EMF at the base frequency, additional EMFs will appear only at rotor slot frequencies $(1 \pm \lambda n\ (1 - s)/p)f_1$ (now, they are time harmonics). Under inter-turn short-circuit conditions a new series of MMF waves will appear, which can be described by the Eq. (13).

$$F_{add}(t,\theta) = \sum_{\substack{k=-\infty \\ k\neq 0}}^{\infty} F_{addk}\cos(\omega_1 t - k\theta) \tag{13}$$

Therefore, there will be MMF and flux-density waves in all numbers of pole pairs and in both directions of rotation of the rotating field. One of these waves has the same number of pole pairs as the basic flux-density wave in the machine, but with an opposite direction of rotation. This wave has no influence on the stator current spectra because it induces only base frequency current component. As previously discussed, all other waves only induce EMFs and generate currents at rotor slot harmonic frequencies. Therefore, no new frequency component appears in the stator current spectra as a result of a fault in the stator windings, only a rise in the rotor slot harmonic frequencies can be expected (Gupta and Culbert, 1993).

These frequency components in $(1 \pm \lambda n(1 - s)/p)f_1$, can also be excited by the phase unbalance. It is required to identify which frequencies will be more sensitive to one or other faults. Now it is possible to make the correct diagnosis in relation to the failure that compromises the motor function.

## 4. EXPERIMENTAL RESULTS

It has been acquired 210 spectra of vibration in a series of 10 tests for each excitement (without fault, two, four, eight and ten turns short circuits, unbalance phase) and randomly repeated under the same load conditions (80, 90 and 100% of load).

The board NI USB-6251 made by National Instruments was used for acquisition data. This board has 16 input analogical channels that can be sampled at up to 200 kHz and 2 digital counters of 24 bits each. The analogical inputs have a 16 bit resolution. The signs of vibration were submitted to an anti-aliasing filter with 2 kHz of cut-off frequency.

The Matlab software was used for the implementation of the algorithm of data acquisition and fault diagnosis.

According to Baccarini, there may be a running time of the motor before the short circuit between turns evolve to short circuit between phase-land and phase to phase, which justifies the development of systems for fault detection.

Through the analysis of items 3.1 and 3.2, it can be said that the presence of an abnormality in the rotor circuit and/or in the stator circuit will provide a disturbance in the vibration that crosses between the air gap machines causing a modification in the reference spectrum.

With the characteristic frequencies of the electric motor, slot harmonic frequencies $(1 \pm \lambda n(1 - s)/p)f_1$ and harmonic of the line frequency $f_l$ ($f_l$ = 60 Hz), 2 $f_l$, 3 $f_l$,. . . , an extremely meticulous study was conducted in order to identify the main frequencies that are excited by the short circuit and unbalance phase.

The spectrum of the vibration for the six poles motor running at a full load condition without fault, short circuit of ten turns and unbalanced phase 200 V is shown in Fig. 6.

After comparing more than 100 spectra of vibration for the six pole motor, it was possible to verify that the 2nd and the 8th harmonic of the line frequency were the most excited because of the insertion of the short circuit and unbalance phase. These harmonics will be considered until the end of the text as being characteristic of the fault frequencies.

For the vibration analysis the graph of tendency for the six pole motor working with 80%, 90% and 100% load is shown in Fig. 7, 8 and 9, respectively.

It was considered that the means of the amplitudes of the fault frequencies characteristics of the ten tests conducted under conditions without fault, two turns short circuit (sc), four turns short circuit, eight turns short circuit, ten turns short circuit and unbalance phase.

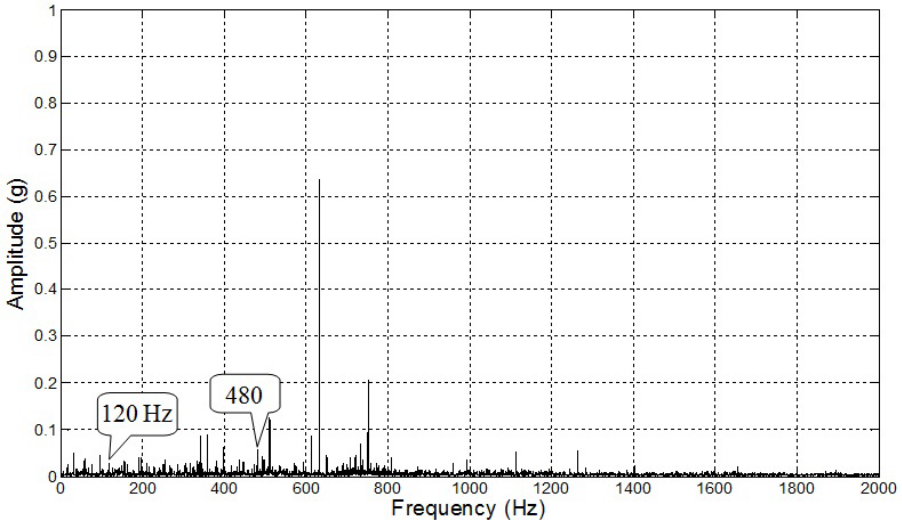


(a) Without fault.

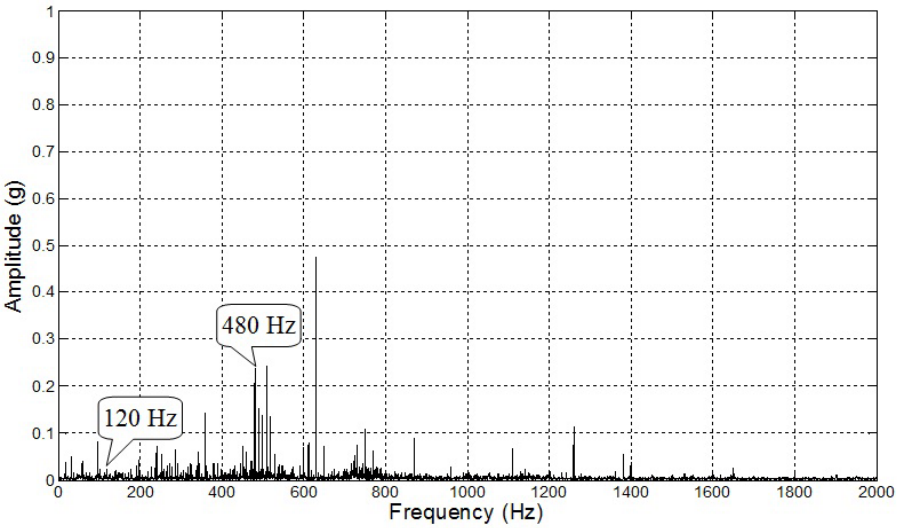


(b) Ten turns short circuited.

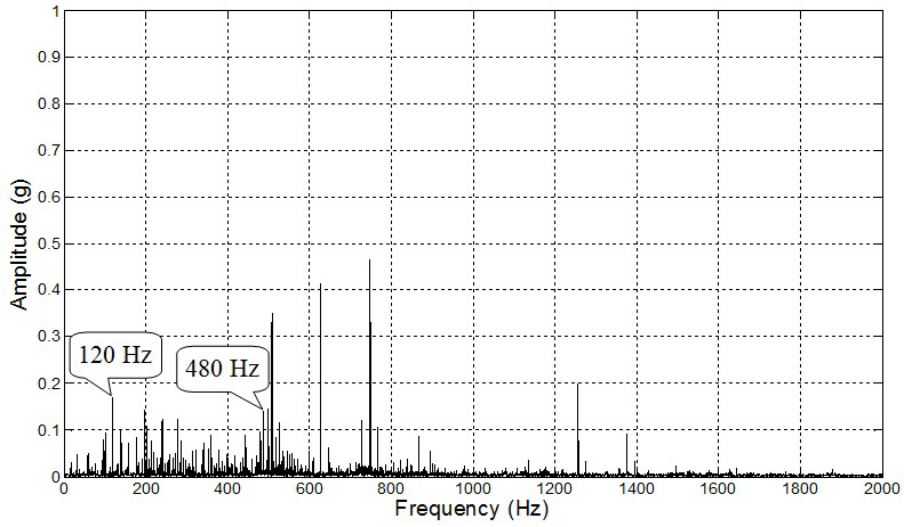


(c) Unbalanced phase 200V.

Figure 6. Six pole induction motor vibration spectra.

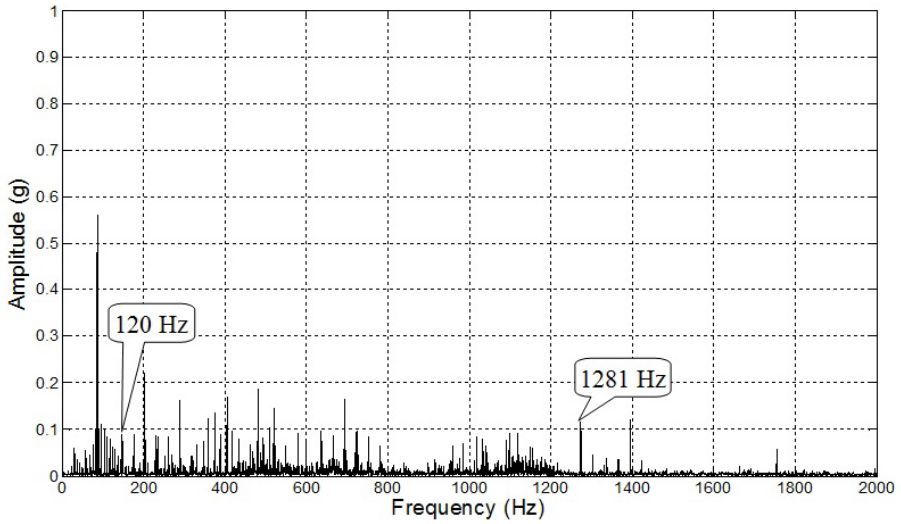


Figure 7. Tendency of the faults introduced into the motor (6 poles) with 80% load.

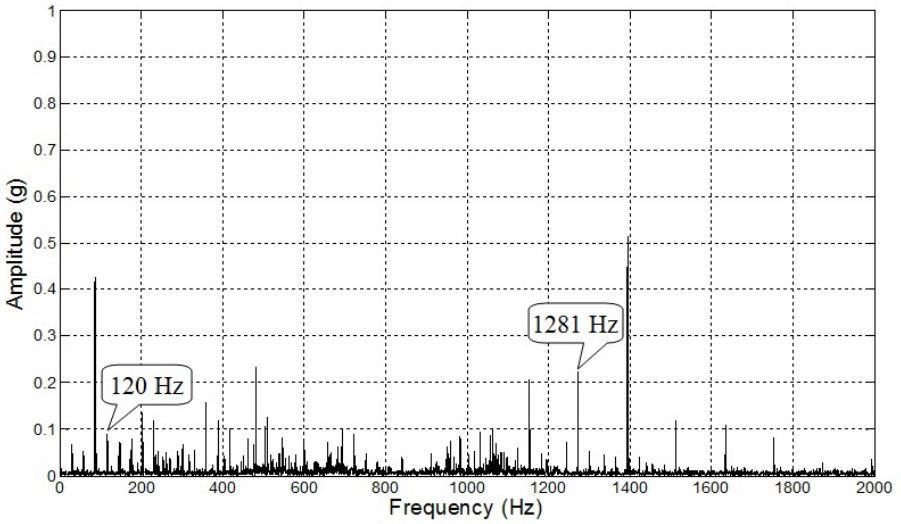


Figure 8. Tendency of the faults introduced into the motor (6 poles) with 90% load.

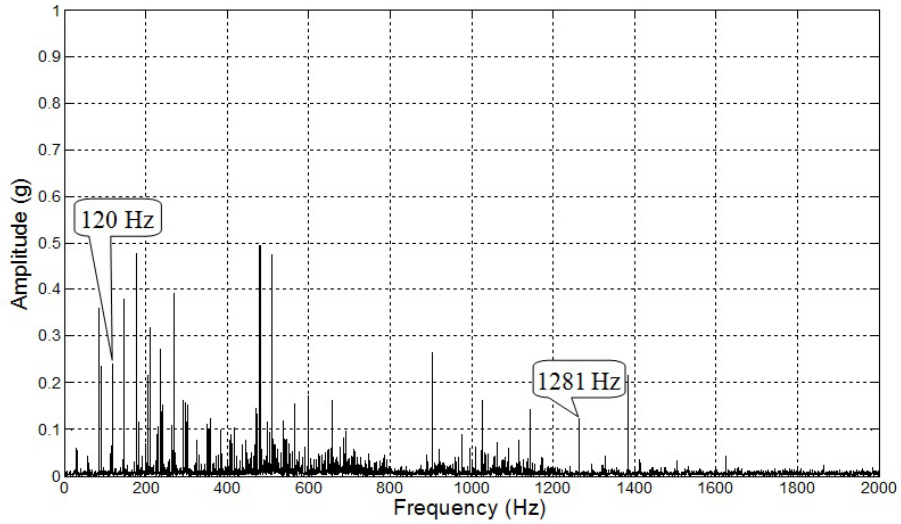


Figure 9. Tendency of the faults introduced into the motor (6 poles) with 100% load.

## 5. CONCLUSION

In this article, we discussed the use of vibration technique to detect and diagnose problems in induction motors from electrical sources (inter-turn short circuits and unbalanced voltage supplies) beyond normal conditions (motor signature). It was observed through the spectra of vibration, that all tests demonstrated a good repeatability and no interference problems of mechanical origin spectra of vibration, ensuring a perfect analysis of the results.

For the short circuit fault, it could be observed that the 8th harmonic of the line frequency was the most excited in the six poles motor. It can be observed gradually from the lower levels that represent only low insulation until higher levels. They can be considered highly detrimental to the good functioning of the machine.

For the failure of the unbalanced voltage supplies, it can be observed that the 2nd harmonic of the line frequency was the most excited in the six poles motors.

It must be highlighted that one of the most important contributions of this work is the relationship between the signals of vibration analysis with some major faults of electric origin (inter-turn short circuits and unbalanced voltage supplies) and the determination of characteristic frequencies of each fault studied in the six poles motors.

The experimental results were undoubtedly impressive and can be adapted and used in real predictive maintenance programs in industries.

## 6. REFERENCES

Baccarini, L. M. R., 2005, "Detectionand diagnose faults in induction motors", Ph.D. thesis, Belo Horizonte, Faculdade de Engenharia Eletrica, Departamento de Engenharia Elétrica, Universidade Federal de Minas Gerais.

Bacacarini, L. M. R., Menezes, B. R. and Caminhas, W. M., 2010, "Fault induction dynamic model, suitable for computer simulation: Simulation results and experimental validation", Machanical Systems and Signal Processing (24) 300-311.

Benbouzid, M. E. H. and Kliman, G. B., 2003, "What stator current processing-based technique to use for induction motor rotor faults diagnosis", IEEE Transactionon Energy Conversion 18 (2) 1078-1084.

Dymond, J. H. and Stranges, N., 2007, "Operation on unbalanced voltage: One motor's experience and more", IEEE Transaction on Industrial Electronics 43 (3) 829-837.

Gupta, B. Y. and Culbert, I. M., 1993, "Assessment of insulation condition in rotating machine stators", IEEE Transaction on Energy Conversion 7 (3) 500-505.

Gojko, M. J. and Penman J., 2000, "The detection of inter-turn short circuits in the windings of operating motors", IEEE on Industrial Electronics 43 (5) 1078-1084.

Henao, H., Demian, C. and Capolino, G. A., 2003, "A frequency-domain detection of stator winding faults in induction machines using an external flux sensor", IEEE Transaction on Industrial Electronics 39 (5) 1272-1279.

Lamim Filho, P. C. M., 2007, "On-line monitoring of three-phase induction motors", Ph.D. thesis, Campinas, Faculdade de Engenharia Mecanica, Departamento de Projetos Mecânicos, Universidade Estadual de Campinas.

Liu, T. and Huang, J., 2005, "A novel method for induction motors stator inter-turn short circuit fault diagnosis by wavelet packet analysis", IEEE Transactions on Electrical Machines and Systems 3 2254 -2258.

Liang, B. and Iwnicki, S. D., 2003, "Asymetrical stator and rotor faulty detection using vibration, phase current and transient speed analysis", Mechanical Systems and Signal Processing 17 (4) 857-869.

Nakamura, H., Oono, T. and Mizuno, Y., 2008, "Analysis of current waveforms of induction motors with short circuit faults", IEEE - Annual Report Conference on Electrical Insulation Dielectric Phenomena 5659.

Silva, A. M., 2006, "Induction motor fault diagnostic and monitoring methods", Master's thesis, Marquette University, Milwaukee, Wisconsin, USA.

Trutt, F. C. and Cruz C. S., 1993, "Prediction of electric behavior in deteriorating induction motors", IEEE Transactions on Industry Application 24 (4) 1239-1243.

Wang, G. F., Li, Y. B. and Luo Z. G., 2009, "Fault classication of rolling bearing based on reconstructed phase space and gaussian mixture model", Journal of Sound and Vibration 323 1077-1089.

Wang, C. and Lai, J. C. S., 1999, "Vibration analysis of an induction motor", Journal of Sound and Vibration 244 (4) 1078-1084.

Widdler Jr., R. D., K. Jr., C. M. and Sudho, S. D., 2006, "An induction motor model for high-frequency torsional vibration analysis", Journal of Sound and Vibration290 865-881.

Zanardelli, W. G., Strangas, E. G., Khalil, H. K. and Miller, J. M., 2005, "Wavelet-based methods for the prognosis of mechanical and eletrical failures in eletric motors", Machanical Systems and Signal Processing (19) 411-426.

## 5. RESPONSIBILITY NOTICE

The authors are the only responsible for the printed material included in this paper.